

## Original Article

# Anticorectal cancer effects and pharmacokinetic application of 2, 2-Bis [4-(4-amino-3-hydroxyphenoxy) phenyl] adamantane

Po-Sheng Yang<sup>1,2\*</sup>, Jane-Jen Wang<sup>3\*</sup>, Tung-Hu Tsai<sup>4</sup>, Yea-Hwey Wang<sup>3</sup>, Woan-Ching Jan<sup>2</sup>, Shih-Ping Cheng<sup>1,2</sup>, Chin-Wen Chi<sup>5</sup>, Yi-Chiung Hsu<sup>6,7</sup>

<sup>1</sup>Department of Surgery, Mackay Memorial Hospital, Mackay Medical College, New Taipei, Taiwan, R. O. C.; <sup>2</sup>Department of Nursing, Mackay Junior College of Medicine, Nursing, and Management, Taipei, Taiwan, R. O. C.; <sup>3</sup>National Taipei University of Nursing and Health Sciences, Taipei, Taiwan, R. O. C.; <sup>4</sup>National Yang-Ming University, School of Medicine, Institute of Traditional Medicine, Taipei, Taiwan, R. O. C.; <sup>5</sup>Department of Medical Research, Taipei Veterans General Hospital, Taipei, Taiwan, R. O. C.; <sup>6</sup>Institute of Statistical Science, Academia Sinica, Taipei, Taiwan, R. O. C.; <sup>7</sup>Department of Horticulture and Biotechnology, Chinese Culture University Taipei, Taiwan, R. O. C. \*Equal contributors.

Received July 13, 2015; Accepted September 1, 2015; Epub September 15, 2015; Published September 30, 2015

**Abstract:** 2, 2-Bis (4-(4-amino-3-hydroxyphenoxy) phenyl) adamantane (DPA) induced growth inhibition in human cancer cells using the national cancer institute (NCI) anticancer drug screen. In our previous study, we demonstrated that DPA exerted growth inhibitory activities in the three human colon cancer cell lines (Colo 205, HT-29, and HCT-15). To identify the detailed mechanism, we examined the functional importance of p21 and p53 in DPA-induced anticancer effect. We used three isogenic colon cancer cell lines, HCT-116, HCT-116 p53<sup>-/-</sup>, and HCT-116 p21<sup>-/-</sup>, to evaluate the roles of p21 and p53 in the *in vitro* anticancer effects of DPA. DPA dose-dependently inhibited cell growth, cell migration and increased cell cycle at the G<sub>0</sub>/G<sub>1</sub> phase in HCT116 cells but not in p21<sup>-/-</sup> and p53<sup>-/-</sup> isogenic HCT-116 cells. Additionally, Western blot showed that DPA treatment induced the p21, p53, and cyclin-E protein expressions in HCT-116 cells. The p21 associated cell cycle regulatory protein such as cyclin D, CDK4, and pRb were decreased after DPA treatment in HCT-116 cells. DPA decreased cell migration in HCT-116 and HCT-116 p53<sup>-/-</sup> but not in HCT-116 p21<sup>-/-</sup> cells. We observed the up-regulation of E-cadherin, p-p38, and p-Erk in DPA-treated HCT-116 group but not in HCT-116 p21<sup>-/-</sup> and HCT-116 p53<sup>-/-</sup> groups. We assumed that p21 was required for DPA-induced anti-colon cancer effect through the Erk and p38 pathway leading to cell cycle arrest and inhibition of cell motility. Mean (± SE) pharmacokinetic parameters of the DPA were as follows: AUC = 64.44 ± 8.41, C<sub>max</sub> = 1.56 ± 0.48 and t<sub>1/2</sub> = 113.92 ± 58.19. The pharmacokinetic data suggest DPA can be applied to further clinical study. This is the first pharmacokinetic study of DPA, and indicated that anti-proliferation and the cell mobility inhibition effects of DPA in HCT116 WT cells may result from the induction of p21 through activation of ERK and p38 pathway.

**Keywords:** Pharmacokinetics, DPA, cell cycle, HCT-116, p21, p53

## Introduction

There were 14.1 million new cancer cases, 8.2 million cancer deaths, 32.6 million people living with cancer (within 5 years of diagnosis), 1.3 million new colorectal cancer cases, 694 thousand deaths due to colorectal cancer and 3.5 million people living with colorectal cancer (within 5 years of diagnosis) in 2012 worldwide. Colorectal cancer (CRC) is the third most common cancer in males and females, which accounts for 8% of new cancer cases in the

United States (US), and is responsible for 8% to 9% of estimated cancer deaths in the US in 2014 [1]. Depending on the stage of CRC, recurrence rates, survival times, and management are different. In early-stage tumors (UICC stage I), radical hemicolectomy with lymph node resection without any additional treatment is appropriate and adjuvant chemotherapy with 5-fluorouracil (5-FU) or capecitabine or the addition of oxaliplatin to the adjuvant treatment can be discussed [2]. Patients with UICC stage III disease (lymph node involvement) should be

## Pharmacokinetic study of anticancer drug DPA

treated with adjuvant chemotherapy (including 5-FU-based regimens and addition of oxaliplatin to a capecitabine regimen) to improve survival [3, 4]. In the metastatic setting, treatment options have emerged from single-agent 5-FU treatment to combination regimens using 5-FU and oxaliplatin or irinotecan or both or with the introduction of targeted substances [2]. These include (A) the anti-vascular endothelial growth factor-A (anti-VEGF-A) antibody bevacizumab, (B) the anti-epidermal growth factor receptor (anti-EGFR) antibodies cetuximab and panitumumab, (C) the anti-angiogenic multi-kinase inhibitor regorafenib, and (D) the anti-angiogenic compound aflibercept. The response rate of current systemic therapies is of ~50%, but resistance develops in nearly all colorectal cancer patients [5] and this is the major obstacle to survival in patients with metastatic chemoresistant colorectal cancer [6]. It is important to develop new drugs for patients with colorectal cancer.

Adamantane derivatives were screened in the National Cancer Institute (NCI) Anticancer Drug Screen system (NSC 706832) [7]. 2, 2-Bis(4-(4-amino-3-hydroxyphenoxy) phenyl) adamantane (DPA) was found to inhibit the growth of several cancer cell lines, especially the colorectal cancer cell line. Our previous study demonstrated that DPA exerted growth inhibitory activities *in vitro* against three human colon cancer cell lines (Colo 205, HT-29, and HCT-15). DPA-treated cells were arrested at G<sub>0</sub>/G<sub>1</sub>, and the DPA-induced cell growth inhibition was irreversible after removal of DPA [8]. Cells showed a more adhesive epithelial phenotype, and the differentiation markers of carcinoembryonic antigen (CEA) and fibronectin (FN) were significantly increased in colon cancer cells after treatment with DPA [8]. The expressions of p21/Cip1, p27/Kip1, E-cadherin, and dephosphorylated p120ctn were involved in DPA-induced anticancer effects [8]. DPA inhibited the growth of human colon cancer cells Colo 205 xenografts, and enhanced the *in vivo* anticancer activity of the chemotherapeutic agent CPT-11 by elevation of p53 independent p21/Cip1 and p27/Kip1 expressions. Moreover, no acute toxicity was observed after an intraperitoneal challenge of DPA in nude mice weekly [8]. These previous results suggest that DPA appears to be a new potentially less toxic modality of cancer combinatory therapy. The goal of this study was to examine the pharma-

cokinetics of DPA and the roles of p21 and p53 in the cellular response against DPA using wild-type, p21<sup>-/-</sup> and p53<sup>-/-</sup> isogenic HCT-116 colon carcinoma cells. We showed here that DPA inhibited cell growth, cell migration and increased cell cycle at the G<sub>0</sub>/G<sub>1</sub> phase in HCT116 cells more than in p21<sup>-/-</sup> and p53<sup>-/-</sup> isogenic HCT-116 cells. The application in pharmacokinetic study of DPA indicates that the area under the plasma concentration versus time curve and elimination half-life were 64.44 ± 8.41 min µg/ml and 113.92 ± 58.19 min, respectively.

### Material and methods

#### *Cell culture and DPA treatment*

*Human colon cancer cell lines:* HCT-116 (ATCC-CCL-247), HCT-116 p53<sup>-/-</sup> and HCT-116 p21<sup>-/-</sup> were grown in McCoy's 5A medium (Sigma-Aldrich, St. Louis, MO) supplemented with 10 µg/ml Pen-Strep-Ampho-Sol. (Biological Industries, Beit Haemek, Israel), 10% fetal bovine serum at 37°C in a humidified atmosphere containing 5% CO<sub>2</sub>. DPA was supplied by Dr. YT Chern [7] and dissolved in DMSO at a stock concentration of 10 mM and added to culture media at a final concentration of 1-6 µM. Cells were seeded at 1.3×10<sup>6</sup> cells/10 cm dish in growth medium containing the DPA. The final concentration of DMSO is 0.1%.

*Sulforhodamine B (SRB) cell proliferation analysis:* Cells seeded at a density of 8000 cells/well in 96-well plates were treated with various doses of DPA for 48 hr. Total biomass of cells was determined by SRB analysis. Briefly, cells were fixed by cold 10% trichloroacetic acid (TCA, Sigma-Aldrich, St. Louis, MO) at 4°C for 1 hr. After washing with tap water and air dried, fixed cells were incubated with 0.1% SRB (Sigma-Aldrich, St. Louis, MO) dissolved in 1% acetic acid for 30 min then rinsed five times with 1% acetic acid to remove unincorporated dye. The protein-bound dye was then extracted with 10 mM Tris (pH 10.5) and the absorbance at 510 nm of this extract was measured by a ELISA reader (Molecular Devices, Sunnyvale, CA).

*Western blotting:* After drug treatment, whole cell pellet were lysed in M-PER reagent (Thermo Scientific, Rockford, IL) with protease inhibitors cocktail (Calbiochem, La Jolla, CA) and phos-

## Pharmacokinetic study of anticancer drug DPA

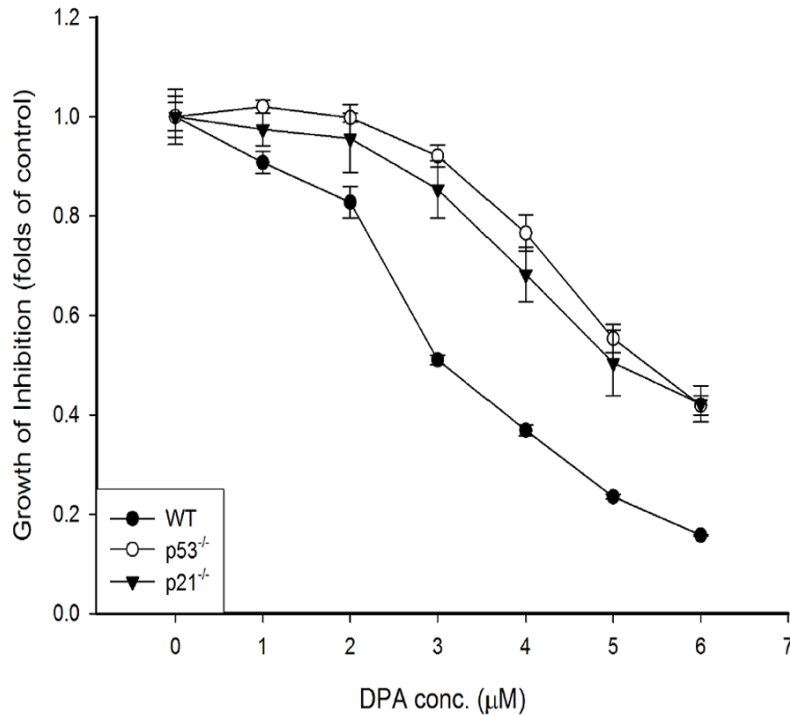


**Figure 1.** Effects of DPA on the growth of HCT-116, HCT-116 p53<sup>-/-</sup> and HCT-116 p21<sup>-/-</sup> cells. Each determination represents mean  $\pm$  SD absorbance of three replicates. The data are representative of three reproducible independent experiments.

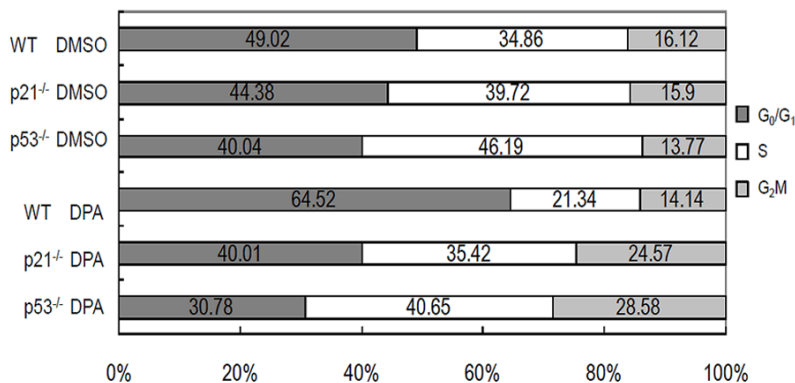


**Figure 2.** Effects of DPA on cell cycle progression of HCT-116, HCT-116 p53<sup>-/-</sup> and HCT-116 p21<sup>-/-</sup> cells. Cells were harvested and processed for cell cycle analysis by flow cytometry after treatment for 48 hr. The results are representative of three independent experiments.

photase inhibitor (Thermo Scientific, Rockford, IL) according to the manufacturer's protocol. Proteins were separated in 10-12% SDS-polyacrylamide gel and transferred to nitrocellulose membranes, blocking in 3% skim milk. After primary antibody incubation at 4°C overnight, the membranes were washed and then incubated with horseradish peroxidase-conju-

gated secondary antibodies. Protein visualization was done using the enhanced chemiluminescence kit (ECL kit, Pierce, Rockford, IL). Primary antibodies: E-cadherin, p21<sup>cip/waf</sup> (BD Biosciences PharMingen, San Diego, CA); p53, cyclin E, cyclin D, CDK2, CDK4, pRb (Santa Cruz Biotechnology Inc., Santa Cruz, CA); pp38, p38, p-ERK, ERK (Cell signaling technology Inc., US);  $\beta$ -Actin (Sigma St. Louis, MO) and  $\alpha$ -tubulin (Millipore, CA). Secondary antibodies: anti-mouse IGG, anti-Rabbit IGG (Millipore, CA).

### Cell cycle analysis

The Cycle TEST Plus DNA Reagent Kit (Becton Dickinson, San Jose, CA) was used for DNA staining. After washing the cells twice with Buffer Solution, the cell concentration was adjusted to  $1.0 \times 10^6$  cells/ml and 0.5 ml of cell suspension was centrifuged at  $400 \times g$  for 5 min at room temperature. The cell pellet was added with 250  $\mu$ l of Solution A (trypsin buffer) and gently mixed. After incubation at room temperature for 10 min, 200  $\mu$ l of Solution B (trypsin inhibitor and RNase buffer) was added to each tube, gently mixed and then incubated at room temperature for 10 min. This was followed by the addition of

200  $\mu$ l of Solution C [propidium iodide (PI) stain solution] and incubated for 10 min in the dark on ice. The sample was filtered through a 50-mm nylon mesh and used for flow cytometric analysis. The red fluorescence (PI) was collected through a 585 nm filter (FL-2) for cell cycle analysis. Data were analyzed using Cellquest and ModFit software on a Macintosh computer.

## Pharmacokinetic study of anticancer drug DPA

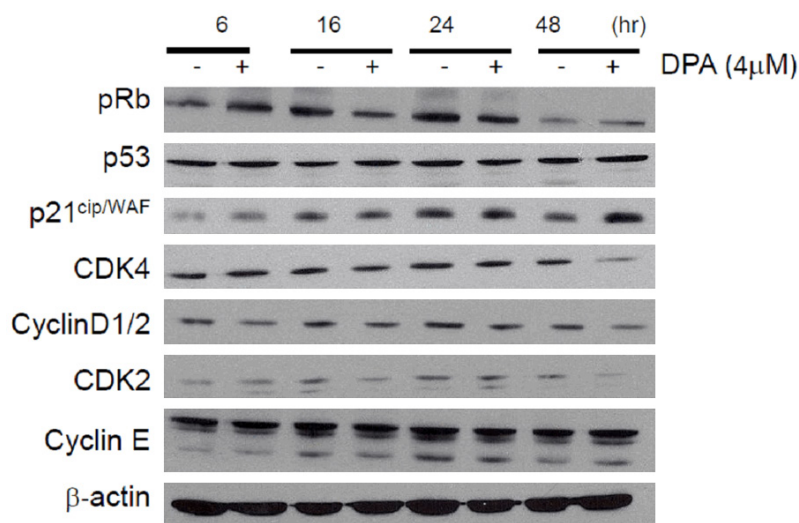


**Figure 3.** The expression of cell cycle related proteins in treated cells. HCT-116 WT cells were treated with 0.1% DMSO (-) or 4  $\mu$ M DPA (+) for 6–48 hr. The actin signal was used for normalization.

### Transwell cell migration analysis

HCT-116, HCT-116 p53<sup>-/-</sup> and HCT-116 p21<sup>-/-</sup> were seeded at  $3 \times 10^5$  cells per 60 mm dish in growth medium. The cells were replenished on the following day with medium containing the vehicle control (0.1% DMSO, Sigma-Aldrich, St. Louis, MO) or DPA (4  $\mu$ M) for 48 hr. Then  $1 \times 10^5$  cells were seeded with 100  $\mu$ l serum-free medium on the top chambers of 24-well transwell plates (8  $\mu$ m pore size, Corning Costar Biosciences, Acton, MA). Growth medium was added to the bottom chambers as the chemoattractant. After incubation for 24 hr, cells on the top surface of transwell insert (non-migrated) were removed by cotton-swab; cells on the bottom surface of the transwell insert (migrated) were fixed by 4% formaldehyde and stained with 0.1% Giemsa solution (Sigma-Aldrich, St. Louis, MO) and photograph was taken using a phase-contrast microscopy and images were captured using AxioVision software (Carl Zeiss, Göttingen, Germany).

### Pharmacokinetic analysis

Pharmacokinetic calculations were carried out using a non-compartmental model with the software WinNonlin Standard Edition Version 1.1 (Scientific Consulting Inc., Apex, NC). The areas under a plot of drug concentration versus time curves (AUC) were calculated according to the log linear trapezoidal method. The clear-

ance of the drug (CL) was calculated as follows:  $CL = \text{dose}/AUC$ . The time required to reduce the drug concentration by half is shown as half-life ( $T_{1/2}$ ) and were expressed as  $T_{1/2} = 0.693/K$ , where K is the first-order rate constant. The mean residence time (MRT) was estimated as  $MRT = AUMC/AUC$ , where AUMC is the area under the first moment curve. All data are presented as mean  $\pm$  SEM.

### Chemicals

Sodium dihydrogen phosphate monohydrate, orthophosphoric acid and HPLC grade solvent were purchased from Merck (Darmstadt, Germany). Triple deionized water (Millipore, Bedford, MA, USA) was used for all preparations. Ibuprofen (RBI, Natick, USA) was used as internal standard and dissolved in acetonitrile.

### Experimental animal

All experimental protocols involving animals were reviewed and approved by the institutional animal experimentation committee of the National Yang-Ming University, Taipei. Male specific pathogen-free Sprague-Dawley rats were obtained from the Laboratory Animal Center of the National Yang-Ming University. The animals had free access to food (Laboratory rodent diet 5P14, PMI Feeds, Richmond, IN, USA) and water until 18 h prior to being used in experiments, at which time only food was removed. Six Sprague-Dawley rats (280–320 g) were under anesthesia (1 ml/kg, i.p. mix with urethane 1 g/ml and  $\alpha$ -chloralose 0.1 g/ml) during the period of surgery and the body temperature of rats was maintained at 37°C with a heating pad.

### Chromatographic conditions

The HPLC system consisted of a Shimadzu corporation (Kyoto, Japan) Model LC-20AT solvent delivery system, a SIL-20 AC auto sampler, a SPD-M20A diode array detector set at 246 nm. DPA and ibuprofen were eluted isocratically at



## Pharmacokinetic study of anticancer drug DPA

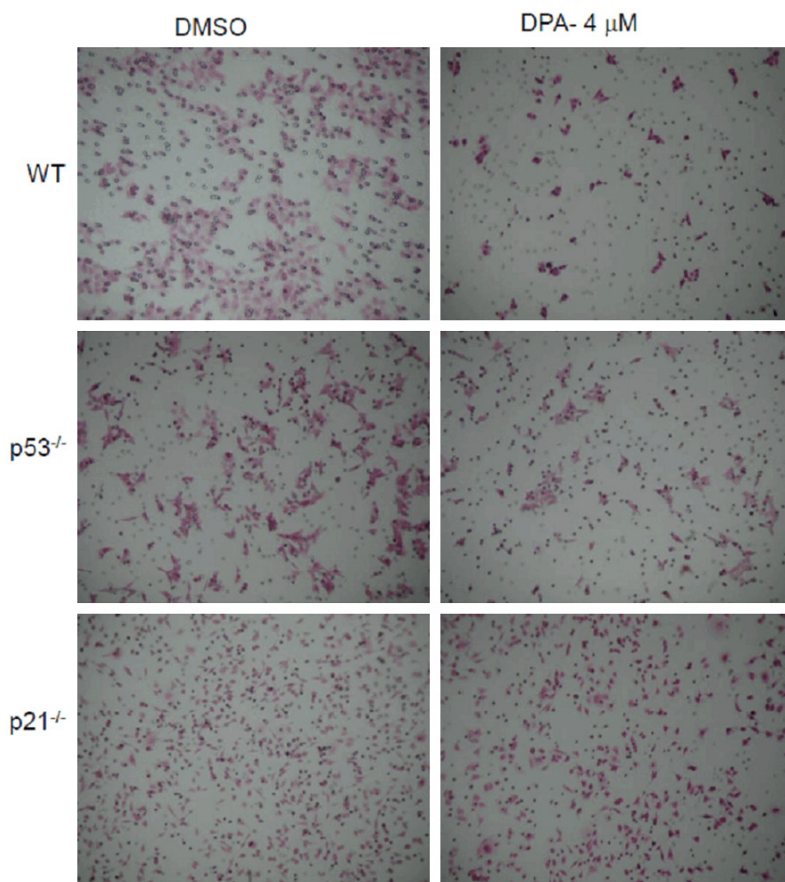


**Figure 4.** Effects of DPA on cell motility of HCT-116, HCT-116 p53<sup>-/-</sup> and HCT-116 p21<sup>-/-</sup> cells. HCT-116, HCT-116 p53<sup>-/-</sup> and HCT-116 p21<sup>-/-</sup> cells were treated with 0.1% DMSO or 4 M DPA for 48 hr, then seeded at a density of 1×10<sup>5</sup> cells/well in 24-well transwell plate and allowed cells migrate for 24 hr. Each condition is assayed in triplicate and the results were reproducible.

ambient temperature and at 1 ml/min with a mobile phase of acetonitrile -20 mM NaH<sub>2</sub>PO<sub>4</sub> (65:35, v/v) (pH 4.3, adjusted by H<sub>3</sub>PO<sub>4</sub>) that had been filtered through a 0.45 μm membrane filter (Millipore). Separation was achieved on an Agilent extended C18 column (4.6×150 mm, 5 μm, Palo Alto, CA, USA).

### Blood sampling and sample preparation

After administrating the DPA (10 mg/kg, i.v.) via femoral vein, the blood samples were directly withdrawn from the rat via heart puncture and collected at 15, 30, 45, 60, 90, 120, 180, 240 and 300 min, respectively. The sampling syringe needles and the collecting eppendorf were rinsed with heparin (15 IU/ml). Every blood sample (0.3 ml) was transferred to the eppendorf and centrifuged at 6000 rpm for 10 min to separate plasma and blood cells. The

resulting plasma sample (60 μl) was vortex-mixed with 120 μl of internal standard solution (ibuprofen, 10 μg/ml). The denatured protein precipitation was separated by centrifugation at 8,000 g for 10 min. An aliquot (20 μl) of the supernatant was directly injected into the HPLC for analysis.

### Statistics

All data are expressed as mean ± SE (standard error). The difference between groups was assessed using Student's t test. A P < 0.05 is considered as significant difference.

### Results

#### Effects of DPA on the growth of HCT-116, HCT-116 p53<sup>-/-</sup>, and HCT-116 p21<sup>-/-</sup>

In our previous research, we have shown that the induction of p21/Cip1, p27/Kip1, E-cadherin and dephosphorylated p120ctn

expression was involved in DPA-induced anti-cancer effects [8]. Interestingly, DPA-induced elevation of p21/Cip1 was independent of the induction of p53 in Colo 205 cells. As shown in **Figure 1**, the growth of HCT-116 cells was reduced 63~85% after exposure to 4~10 μM DPA for 48 hr, while the growth of HCT-116 p53<sup>-/-</sup> and HCT-116 p21<sup>-/-</sup> cells only had about 30~60% reduction. The growth of HCT-116 cells was much more sensitive to DPA than HCT-116 p53<sup>-/-</sup> or p21<sup>-/-</sup> cells.

#### Effects of DPA on the cell cycle progression of HCT-116, HCT-116 p53<sup>-/-</sup>, and HCT-116 p21<sup>-/-</sup>

For investigation of the effect of DPA on cell cycle progression cells were stained by PI and measured by flow cytometry at 48 hr following 4 μM DPA drug treatments. In **Figure 2**, as compare to DMSO control, DPA increased the per-

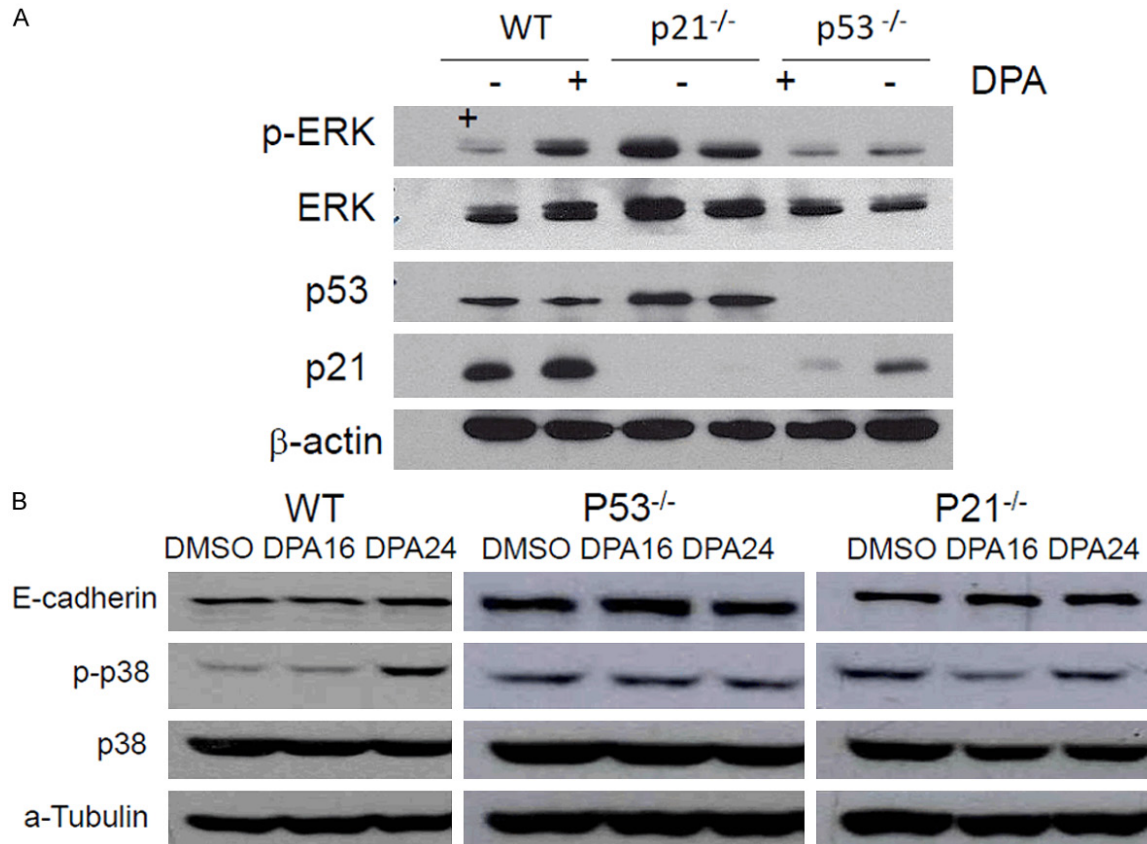


**Figure 5.** A. Immunoblot analysis of p-ERK, ERK, p21 and p53 in treated cells. HCT-116, HCT-116 p21<sup>-/-</sup> and HCT-116 p53<sup>-/-</sup> cells were treated with 0.1% DMSO (-) or 4 M DPA (+) for 48 hr. The Actin signal was used for normalization. B. The expression of E-cadherin, p38 and p-p38 in treated cells. HCT-116, HCT-116 p21<sup>-/-</sup> and HCT-116 p53<sup>-/-</sup> cells were treated with 0.1% DMSO or 4 M DPA for 16 hr (DPA16) and 24 hr (DPA24). The tubulin signal was used for normalization.

centage of G<sub>0</sub>/G<sub>1</sub> phase (64.52% vs. 49.02%) cells and reduced the cells in S (21.34% vs. 34.86%) phase of HCT-116 cells. DPA increased the percentage of G<sub>0</sub>/G<sub>1</sub> phase cells and reduced the cells in S phase on HCT-116 cells, and these effects were not observed on DPA-treated HCT-116 p53<sup>-/-</sup> and HCT-116 p21<sup>-/-</sup> cells. These results suggested that the p21 and p53 were involved in DPA-induced HCT-116 cells arrest in G<sub>0</sub>/G<sub>1</sub> phase.

*Changes in cell cycle related proteins on HCT-116 cells after DPA treatment*

In previous experiment, we confirmed that DPA decreased the cell growth, and the cell cycle was arrest in G<sub>0</sub>/G<sub>1</sub> phase in HCT-116 cells, but not in HCT116 p21<sup>-/-</sup> and HCT116 p53<sup>-/-</sup> cells. Further, to examine the cell cycle related proteins involved in the G<sub>0</sub>/G<sub>1</sub> phase arrest in HCT116 cells after 4 μM DPA treatment for 6~48 hr, we harvested cells for Western blotting. We observed the up-regulation of p21, and

down-regulation of pRb, CDK2 and cyclin D/CDK4 in the DPA-treated groups (Figure 3). The p53 and cyclin E showed no significant difference between the DPA-treated and control groups.

*Effects of DPA on cell migration of HCT-116, HCT-116 p53<sup>-/-</sup>, and HCT-116 p21<sup>-/-</sup> cells*

To investigate the DPA effect on cell migration of colon cancer cells, we used transwell migration assay. As shown in Figure 4, the motility was decreased in 4 μM DPA treated-HCT-116 and HCT-116 p53<sup>-/-</sup> cells, but no effect was observed on the migration of DPA treated-HCT-116 p21<sup>-/-</sup> cells.

*The expression of cell migration-related proteins on DPA-treated HCT-116, HCT-116 p53<sup>-/-</sup> and HCT-116 p21<sup>-/-</sup>*

Further, to identify the role of p21, p53 and related proteins involved in the migration inhibition in HCT-116 cells after DPA treatment, we

## Pharmacokinetic study of anticancer drug DPA

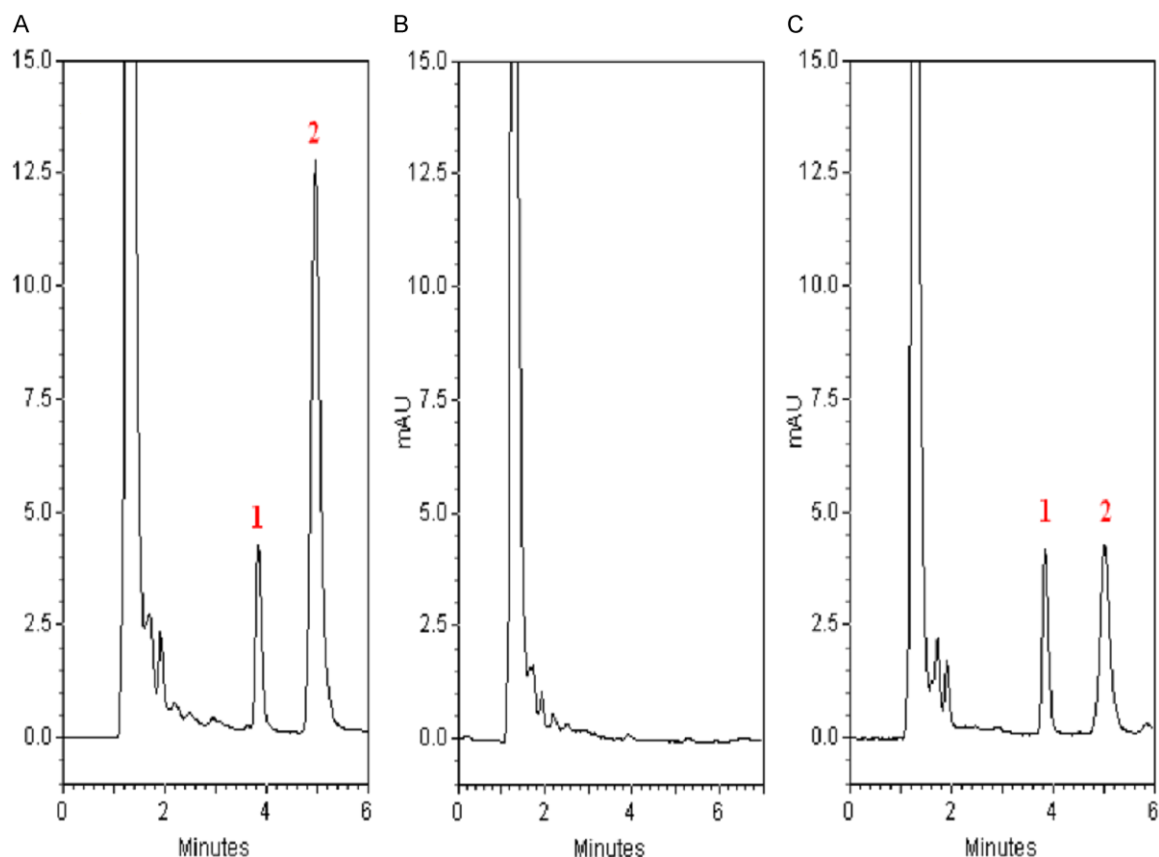


**Figure 6.** Typical chromatograms of (A) standard DPA spiked (5 µg/mL) in rat plasma, (B) Blank plasma sample before drug administration, and (C) plasma sample containing DPA (1.68 µg/mL) collected from the rat plasma 15 min after DPA administration (10 mg/kg, i.v.). 1: internal standard (10 µg/mL), 2: DPA.

examined E-cadherin, p-ERK, and p-p38 expression level in HCT-116, HCT-116 p21<sup>-/-</sup>, and HCT-116 p53<sup>-/-</sup> cells. We observed the up-regulation of E-cadherin, p-p38, and p-Erk in DPA-treated HCT-116 cells but not in HCT-116 p21<sup>-/-</sup> and HCT-116 p53<sup>-/-</sup> cells (Figure 5). We presumed that the expression of E-cadherin and the activation of Erk and p38 pathway were p21 and p53 dependence.

### Pharmacokinetic application of DPA

The separations of DPA from endogenous interfering species and quantitation using the internal standard ibuprofen with the present chromatographic conditions are adequate. The chromatograms acquired at 246 nm absorbance wavelength with the injection of plasma samples all show stable baselines and reproducible DPA and internal standard peaks. This wavelength at 246 nm is the optimal maximum absorbance position at DPA spectrum determined with the photodiode array. Typically the

chromatographic peaks of internal standard (ibuprofen) and DPA appear at 4.3 and 5.1 min respectively. These two peaks are separated from endogenous species eluted less than 6 min. Figure 6A shows the chromatogram of a standard of DPA spiked in plasma (5 µg/ml). Figure 6B shows the chromatogram of a drug-free plasma extract, which illustrates a clean, stable baseline with endogenous peaks eluted before 6 min. Figure 6C shows the chromatogram of a plasma sample containing DPA (1.68 µg/ml) collected from a rat plasma 15 min after DPA administration (10 mg/kg, i.v.), and no peak distortions were visible. Each determination was completed within 6 min and no carry-over peaks were detected in subsequent chromatograms of plasma samples. At the range 0.1-5 µg/ml in rat plasma, the concentration of DPA is linearly proportional to its chromatographic peak area, corrected with the peak area of internal standard on the same chromatogram. The limit of detection of DPA in rat plasma is determined to be 30 ng/ml at a sig-

## Pharmacokinetic study of anticancer drug DPA

**Table 1.** Method validation for the intra-assay and inter-assay precision (% RSD) and accuracy (% Bias) of the method for the determination of DPA in rat plasma

Nominal concentration (µg/ml)	Observed concentration (µg/ml)	RSD (%)	Accuracy bias (%)
Inter assay			
0.1	0.10 ± 0.02	17.13	0.44
0.5	0.50 ± 0.02	4.26	0.61
1	0.99 ± 0.01	0.86	-0.38
5	5.00 ± 0.00	0.03	0.01
Intra assay			
0.1	0.11 ± 0.01	13.09	7.66
0.5	0.49 ± 0.01	2.67	-1.81
1	1.00 ± 0.01	1.21	0.1
5	5.00 ± 0.00	0.05	0.01

nal-to-noise ratio of 3. The lower limit of quantitation (LOQ) is 0.1 µg/ml.

The intra- and inter-assay precision and accuracy values are evaluated at the concentration range of 0.1-5 µg/ml (**Table 1**). The overall precision, defined by the relative standard deviation (RSD), range from 0.03 to 17.13% in average. Analytical accuracy, expressed as the percentage difference between the mean of measured value and the known concentration vary from -1.81 to 7.66%. The extraction recovery of DPA in rat plasma was  $94.0 \pm 1.6\%$ . This method was developed for the application in pharmacokinetic study of DPA in anesthetized rat. **Figure 7** illustrates the concentration versus time profiles of DPA with a single intravenous dose administration to one group of six individual rats. Pharmacokinetic calculations were performed on each individual set of data using the pharmacokinetic software WinNonlin Standard Edition Version 1.1 (Pharsight Corp., Mountain View, CA, USA) by non-compartmental method. Our result indicates that the area under the plasma concentration versus time curve and elimination half-life were  $64.44 \pm 8.41$  min µg/ml and  $113.92 \pm 58.19$  min, respectively (**Table 2**).

### Discussion

From this study, we found that DPA dose-dependently inhibited cell growth, cell migration and increased cell cycle at the  $G_0/G_1$  phase in HCT116 cells more than in p21<sup>-/-</sup> and p53<sup>-/-</sup> isogenic HCT-116 cells. Using HPLC-diode array

**Table 2.** Pharmacokinetic data after DPA administration (10 mg/kg, i.v.) in rats

Pharmacokinetic parameters	10 mg/kg
C <sub>max</sub> (µg/ml)	1.56 ± 0.48
T <sub>1/2</sub> (min)	113.92 ± 58.19
AUC (min µg/ml)	64.44 ± 8.41
CL (ml/min/kg)	123.38 ± 23.07
MRT (min)	127.63 ± 48.63

detection method developed in this study, DPA was successfully separated from plasma samples in anesthetized rat. After optimizing the detection conditions, experiments were conducted to improve the chromatographic separation of the analyses. Good linearity was achieved in the range of 0.1-5.0 µg/mL. There was no interference under the present analytical conditions of DPA in rat plasma. The accuracy and precision of the concentrations were all acceptable. Our data suggest DPA can be further applied to clinical study based on our solid pharmacokinetic data.

Analyte matrix effect and recovery were used to evaluate different sample preparations, while the post-column infusion method and the post-extraction spike method were used to evaluate matrix effects [9]. In this study, the post-extraction spike method was selected to evaluate the matrix effect of DPA in plasma samples. This method quantitatively evaluates matrix effects by contrasting the response of an analyte in standard solution to the response of the analyte spiked into a blank matrix sample that has been passed through the sample preparation process.

The pharmacokinetic curve showed that the mean plasma concentration was distributed during the first 120 min and then trends toward excretion for the later 180 min, indicating that DPA displays regular distribution and elimination phase after DPA administration. However, we could not detect DPA in plasma up to six hours after a single dose was administered. These results propose that the analytical method was very repeatable and reliable base on the intra- and inter-assay precision and accuracy performed by our analytical system. Whether DPA alone and/or its metabolites could distribute to specific organ(s) needs further elucidation.



## Pharmacokinetic study of anticancer drug DPA

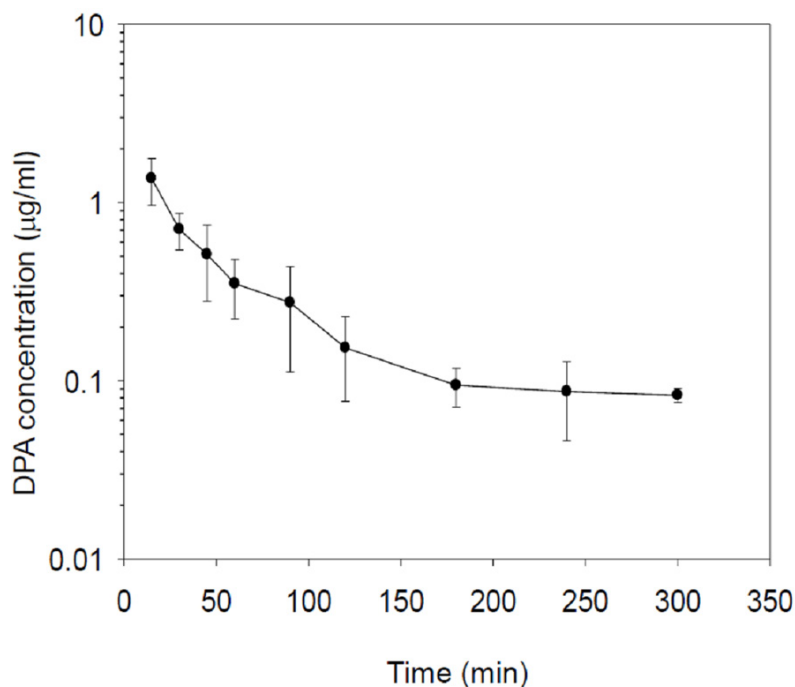


**Figure 7.** Mean concentration-time profiles of DPA in rat plasma after DPA administration (10 mg/kg, i.v.). Each point represents the mean  $\pm$  S.E. for six rats.

DPA is one kind of adamantane derivatives which possess several attractive pharmacological activities, such as antibacterial, antifungal, antiviral and anticancer effects [10-13]. Our previous study found that N-1-adamantyl-citraconimide, N-1-adamantylmaleimide (AMI) and N-1-diamantylmaleimide (DMI) exhibited modest growth-inhibitory activity against four cancer cell lines (Colo 205, HepG2, SK-BR-3 and Molt-4) [14]. We also found that AMI was effective in inhibiting the growth of human gastric cancer cells both *in vitro* and *in vivo* and induced apoptosis *in vitro* [15]. The AMI derivative dimethyladamantylmaleimide (DMAMI) induces apoptosis and inhibits the growth of human colon cancer Colo 205 in SCID mice [13]. The *in vitro* antitumor activities of DPA were screened against the National Cancer Institute (NCI)'s 60 human cancer cell lines. DPA exhibited marked anticancer activity on colon cancer cell lines, and induced G1 arrest in Colo 205 and HT-29 cells [7, 16]. These results suggest that compounds with adamantyl substituent t have more potent anticancer activities, and are worthy to consider as highly promising candidate in drug design. We previously demonstrated that DPA is active in inhibiting the growth of human colon cancer cells

Colo 205, HT-29 and HCT-15 [8]. DPA-treated cells showed a more adhesive epithelial phenotype. The differentiation markers of carcinoembryonic antigen (CEA) and fibronectin (FN) were significantly increased in colon cancer cells after treatment with DPA. Further studies showed the induction of p21/Cip1, p27/Kip1, E-cadherin and dephosphorylated p120ctn expression was involved in DPA-induced anticancer effects. DPA-induced elevation of p21/Cip1 was independent of the induction of p53 in Colo 205 cells. The tumor suppressor has been implicated in a variety of cellular processes [17]. Among the transcriptional targets of p53, the CDKI p21/Cip1 plays a key role in mediating

G1 arrest [18]. In this study, DPA increased the percentage of G<sub>0</sub>/G<sub>1</sub> phase cells and reduced the cells in S and G2M phase of HCT-116 wild-type cells. In contrast, such effect was not observed on HCT-116 p53<sup>-/-</sup> and HCT-116 p21<sup>-/-</sup> cells (**Figure 2**). It is reasonable to conclude that DPA induced G1 arrest through p21 and p53. Regulation of cell-cell and cell-extracellular matrix (ECM) interaction is important for development, regeneration, tumor progression and, particularly, invasion and metastasis [19, 20]. Reduced cell-cell adhesiveness is associated with loss of contact inhibition of proliferation, thereby allowing escape from growth control signals [21]. From our previous study [8], DPA-induced differentiation in Colo 205, HT-29 and HCT-15 colon cancer cells was associated with an increased production of CEA and FN, and DPA-treated cells showed a more adhesive epithelial phenotype. The expression of p21/Cip1, p27/Kip1, E-cadherin,  $\beta$ -catenin and p120 was involved in DPA-induced *in vitro* cytostatic and differentiation effects. In this study as shown in **Figure 3**, the motility was decreased in DPA treated-HCT-116 and HCT-116 p53<sup>-/-</sup> cells, but had no effect on the migration of DPA treated-HCT-116 p21<sup>-/-</sup> cells. Further we investigated the migration

associated protein; E-cadherin was also enhanced in DPA-treated HCT-116 WT cells but no effect in HCT-116 p21<sup>-/-</sup> cells. From these results we confirmed that p21 is an important regulator of cell movement. P21 is an important cell cycle regulator induced via the activation of p53-dependent or p53-independent pathway, or RAF-MEK-ERK pathway [22, 23]. Some studies showed that p21 induction is an important indicator of growth inhibition in colorectal cancer cells [24]. The p21 activation was identified as a marker for ERK pathway dependent anti-proliferation [25, 26]. ERK1/2 and p38 cooperate to induce a p21<sup>CIP1</sup>-dependent G1 cell cycle arrest [27]. Our data identified that anti-proliferated and the cell mobility inhibition effects of DPA in HCT-116 cells may result from the induction of p21 through activation of ERK or p38 pathway.

#### Acknowledgements

Dr. Y-T CHERN (Department of Chemical Engineering, National Taiwan University of Science and Technology, Taipei).

#### Disclosure of conflict of interest

None.

**Address correspondence to:** Dr. Yi-Chiung Hsu, Institute of Statistical Science, Academia Sinica, Taipei 115, Taiwan, R. O. C. Tel: 886-2-27835611 Ext. 438; Fax: 886-2-27831523; E-mail: syic@stat.sinica.edu.tw; Dr. Po-Sheng Yang, Department of Surgery, Mackay Memorial Hospital, Mackay Medical College, New Taipei, Taiwan, R. O. C. E-mail: psyangd0039@gmail.com

#### References

- [1] Siegel R, Ma J, Zou Z and Jemal A. Cancer statistics, 2014. *CA Cancer J Clin* 2014; 64: 9-29.
- [2] Stintzing S. Management of colorectal cancer. *F1000Prime Rep* 2014; 6: 108.
- [3] Haller DG, Tabernero J, Maroun J, de Braud F, Price T, Van Cutsem E, Hill M, Gilberg F, Rittweger K and Schmoll HJ. Capecitabine plus oxaliplatin compared with fluorouracil and folinic acid as adjuvant therapy for stage III colon cancer. *J Clin Oncol* 2011; 29: 1465-1471.
- [4] Andre T, Boni C, Mounedji-Boudiaf L, Navarro M, Tabernero J, Hickish T, Topham C, Zaninelli M, Clingan P, Bridgewater J, Tabah-Fisch I, de Gramont A; Multicenter International Study of Oxaliplatin/5-Fluorouracil/Leucovorin in the Adjuvant Treatment of Colon Cancer (MOSAIC) Investigators. Oxaliplatin, fluorouracil, and leucovorin as adjuvant treatment for colon cancer. *N Engl J Med* 2004; 350: 2343-2351.
- [5] Dallas NA, Xia L, Fan F, Gray MJ, Gaur P, van Buren G 2nd, Samuel S, Kim MP, Lim SJ and Ellis LM. Chemoresistant colorectal cancer cells, the cancer stem cell phenotype, and increased sensitivity to insulin-like growth factor-I receptor inhibition. *Cancer Res* 2009; 69: 1951-1957.
- [6] Dy GK, Hobday TJ, Nelson G, Windschitl HE, O'Connell MJ, Alberts SR, Goldberg RM, Nikcevic DA and Sargent DJ. Long-term survivors of metastatic colorectal cancer treated with systemic chemotherapy alone: a north central cancer treatment group review of 3811 patients, n0144. *Clin Colorectal Cancer* 2009; 8: 88-93.
- [7] Wang JJ, Chen YC, Chi CW, Huang KT and Chern YT. In vitro and in vivo growth inhibition and G1 arrest in human cancer cell lines by diaminophenyladamantane derivatives. *Anti-cancer Drugs* 2004; 15: 697-705.
- [8] Wang JJ, Lee JY, Chen YC, Chern YT and Chi CW. The antitumor effect of a novel differentiation inducer, 2, 2-Bis (4-(4-amino-3-hydroxyphenoxy) phenyl) adamantane (DPA), in combinatory therapy on human colon cancer. *Int J Oncol* 2006; 28: 1003-1012.
- [9] Chambers E, Wagrowski-Diehl DM, Lu Z and Mazzeo JR. Systematic and comprehensive strategy for reducing matrix effects in LC/MS/MS analyses. *J Chromatogr B Analyt Technol Biomed Life Sci* 2007; 852: 22-34.
- [10] Aigami K, Inamoto Y, Takaishi N, Hattori K and Takatsuki A. Biologically active polycycloalkanes. 1. Antiviral adamantane derivatives. *J Med Chem* 1975; 18: 713-721.
- [11] Tverdislov VA, el-Karadagi S, Kharitonov IG, Glaser R, Donath E, Herrmann A, Lentzsch P and Donath J. Interaction of the antiviral agents remantadine and amantadine with lipid membranes and the influence on the curvature of human red cells. *Gen Physiol Biophys* 1986; 5: 61-75.
- [12] Chen HS, Pellegrini JW, Aggarwal SK, Lei SZ, Warach S, Jensen FE and Lipton SA. Open-channel block of N-methyl-D-aspartate (NMDA) responses by memantine: therapeutic advantage against NMDA receptor-mediated neurotoxicity. *J Neurosci* 1992; 12: 4427-4436.
- [13] Wang JJ, Chern YT, Chang YF, Liu TY and Chi CW. Dimethyladamantylmaleimide-induced in vitro and in vivo growth inhibition of human colon cancer Colo205 cells. *Anticancer Drugs* 2002; 13: 533-543.
- [14] Wang JJ, Wang SS, Lee CF, Chung MA and Chern YT. In vitro antitumor and antimicrobial activities of N-substituents of maleimide by

## Pharmacokinetic study of anticancer drug DPA

- adamantane and diamantane. *Chemotherapy* 1997; 43: 182-189.
- [15] Wang JJ, Chern YT, Liu TY and Chi CW. In vitro and in vivo growth inhibition of cancer cells by adamantylmaleimide derivatives. *Anticancer Drug Des* 1998; 13: 779-796.
- [16] Wang JJ, Huang KT and Chern YT. Induction of growth inhibition and G1 arrest in human cancer cell lines by relatively low-toxic diamantane derivatives. *Anticancer Drugs* 2004; 15: 277-286.
- [17] Bates S and Vousden KH. p53 in signaling checkpoint arrest or apoptosis. *Curr Opin Genet Dev* 1996; 6: 12-18.
- [18] Waldman T, Kinzler KW and Vogelstein B. p21 is necessary for the p53-mediated G1 arrest in human cancer cells. *Cancer Res* 1995; 55: 5187-5190.
- [19] Hynes RO and Lander AD. Contact and adhesive specificities in the associations, migrations, and targeting of cells and axons. *Cell* 1992; 68: 303-322.
- [20] Liotta LA, Steeg PS and Stetler-Stevenson WG. Cancer metastasis and angiogenesis: an imbalance of positive and negative regulation. *Cell* 1991; 64: 327-336.
- [21] St Croix B, Sheehan C, Rak JW, Florenes VA, Slingerland JM and Kerbel RS. E-Cadherin-dependent growth suppression is mediated by the cyclin-dependent kinase inhibitor p27 (KIP1). *J Cell Biol* 1998; 142: 557-571.
- [22] Liu Y, Martindale JL, Gorospe M and Holbrook NJ. Regulation of p21WAF1/CIP1 expression through mitogen-activated protein kinase signaling pathway. *Cancer Res* 1996; 56: 31-35.
- [23] Kerkhoff E and Rapp UR. Cell cycle targets of Ras/Raf signalling. *Oncogene* 1998; 17: 1457-1462.
- [24] Kim JA, Park KS, Kim HI, Oh SY, Ahn Y, Oh JW and Choi KY. Troglitazone activates p21Cip/WAF1 through the ERK pathway in HCT15 human colorectal cancer cells. *Cancer Lett* 2002; 179: 185-195.
- [25] Park KS, Ahn Y, Kim JA, Yun MS, Seong BL and Choi KY. Extracellular zinc stimulates ERK-dependent activation of p21(Cip/WAF1) and inhibits proliferation of colorectal cancer cells. *Br J Pharmacol* 2002; 137: 597-607.
- [26] Park KS, Jeon SH, Oh JW and Choi KY. p21Cip/WAF1 activation is an important factor for the ERK pathway dependent anti-proliferation of colorectal cancer cells. *Exp Mol Med* 2004; 36: 557-562.
- [27] Todd DE, Densham RM, Molton SA, Balmanno K, Newson C, Weston CR, Garner AP, Scott L and Cook SJ. ERK1/2 and p38 cooperate to induce a p21CIP1-dependent G1 cell cycle arrest. *Oncogene* 2004; 23: 3284-3295.